10thInternational Conference on Fracture Mechanics of Concrete and Concrete Structures
FraMCoS-X
G. Pijaudier-Cabot, P. Grassl and C. La Borderie (Eds)
https://doi.org/10.21012/FC10.229373

STRENGTH CRITERION FOR SIZE EFFECT ON QUASI-BRITTLE FRACTURE WITH AND WITHOUT NOTCH

YI CHEN[*], XIANGYU HAN[*†], XIAOZHI HU[*††], BINHUA WANG[††] AND WANCHENG ZHU[†††]

[*]University of Western Australia
Department of Mechanical Engineering
Perth, WA6009, Australia
e-mail: xiao.zhi.hu@uwa.edu.au

[†]Southwest Jiaotong University
Key Laboratory of Transportation Tunnel Engineering, MOE
Chengdu 610031, PR China

[††]Chang'an University
Key Laboratory of Road Construction Technology and Equipment, MOE
Xi'an 710064, PR China
e-mail: wangbh@chd.edu.cn

[†††]Northeastern University
School of Civil Engineering
Shenyang 110809, PR China
e-mail: zhuwancheng@mail.neu.edu.cn

Key words: Size Effect, Boundary Effect, Tensile Strength, Statistical Fracture, Grain Size

Abstract: This study shows it is sufficient to use only the tensile strength f_t to describe the size effect on quasi-brittle fracture behaviors of brittle heterogeneous solids such as rock and concrete. Another essential material property, the average grain size G for rock or the maximum aggregate size d_{max} for concrete, should be determined separately before fracture analysis. Quasi-brittle fracture behaviors of heterogeneous specimens or structures, small or large and notched or un-notched, can all be described by the "one-parameter f_t criterion" evolved from the boundary effect model (BEM). Using the mean and standard deviation from normal distribution analysis of test data, the simplified BEM can predict the mean quasi-brittle fracture curve and statistical scatters with 95% reliability, covering the entire fracture range from the strength f_t criterion to the fracture toughness K_{IC} criterion (LEFM), and the quasi-brittle fracture region in-between. K_{IC} is fully determined by f_t and G, making the one-parameter f_t approach possible. This one-parameter approach thus requires only "one measurement" from a group of specimens of any size with any notch length. The 95% reliability band established statistically can be conveniently used in design applications.

1 INTRODUCTION

Size effect on quasi-brittle fracture of heterogeneous solids such as concrete and rock have been commonly modelled by two separate size effect laws (SEL), depending on whether specimens are notched or un-notched [1, 2]. This is because SEL is strictly limited to geometrically similar specimens, i.e. the notch/specimen-size ratio ($a_0/W = \alpha$-ratio) has

to be constant. Therefore, separate curve-fitting is always required if different α-ratios are involved, e.g. notched (α = 0.1, 0.2 ...) and un-notched (α = 0). Furthermore, the two SELs have different parameters and formulae [1, 2].

The most widely-used SEL [3] is also the simplest for specimens with "deep notch", typically with α-ratio > 0.1. For un-notched specimens, there are two different forms of SEL, thus more parameters, depending on whether Weibull size effect is considered or not. Therefore, we have two SELs for un-notched cases, one SEL for deep-notch cases.

This study adopts the boundary effect model (BEM) for size effect study because BEM [4-7] can be rearranged into one simple closed-form solution, which has all the intended functions of those three SELs.

Results of a granite with the average grain size G around 2 mm and a medium-grained sandstone with G around 0.3 – 0.4 mm are analysed by the simplified BEM. Concrete results with the maximum aggregate d_{max} = 10 mm [1, 8-10] are also assessed for comparison. To assist young researchers, students and design engineers, advantages and disadvantages of SEL and BEM are discussed so that they can purposely select suitable models for their specific cases.

2 f_t & SIMPLIFIED BEM

The average grain size G, a key material microstructure property, for rock and ceramics should be measured separately prior to fracture test and analysis. The maximum aggregate size d_{max} is readily available for a concrete mix.

Recently, the grain size G or d_{max} has been included in BEM analysis [6, 7], and linked to the crack-bridging zone Δa_{fic} behind the fictitious crack tip, at which the stress is equal to f_t.

$$\Delta a_{fic} \approx 1.5 \cdot G \approx 1.0 \cdot d_{max} \tag{1}$$

This approximation for the through-the-thickness fictitious crack growth (a real crack front is not straight, and part of it may be 1.0·G or 2.0·G) is based on the assumption that crack growth in heterogeneous solids with coarse microstructures takes place in a stepwise manner. A discrete number is thus introduced in [6, 7], linking the fictitious crack growth to the grain size (or aggregate size), which can vary by 0.5 interval (or rougher by 1.0), i.e. 0.0, 0.5, 1.5, 2.0 etc. Considering the most likely "stepwise cracking" in heterogeneous solids, Eq. (1) is a reasonable approximation for common small three-point-bending (3-p-b) specimens with the W/G ratio varying from 5 to 50.

From the early work of Hillerborg [11], the characteristic length l_{ch} is known to be linked to the material microstructures, i.e. l_{ch} of concrete is larger than that of mortar. The characteristic crack a_{ch}^* introduced in BEM [4, 7] is proportional to l_{ch}. From a wide range of ceramic and concrete data, we have obtained the following approximation [12-14], again with 0.5 interval for the discrete number.

$$a_{ch}^* \approx 3.0 \cdot G \tag{2}$$

Substituting those two approximations into the final equation in [6, 7], the following closed-form solution is obtained, e.g. [10, 13, 14].

$$\begin{aligned} P_{max} &= f_t \cdot A_e\left(W,\, a_0,\, G\right) \\ &= f_t \cdot \frac{\left(W - a_0\right)\left(W - a_0 + 2\Delta a_{fic}\right)}{1.5\left(\frac{S}{B}\right)\sqrt{1 + \frac{a_e}{a_{ch}^*}}} \\ &= f_t \cdot \frac{W^2\left(1-\alpha\right)\left(1 - \alpha + \frac{3G}{W}\right)}{1.5\left(\frac{S}{B}\right)\sqrt{1 + \frac{a_e}{3G}}} \end{aligned} \tag{3}$$

The equation for concrete using d_{max} can be obtained easily by substituting the relation between G and d_{max} in Eq. (1). A_e in Eq. (3) is an equivalent area measurement, i.e. Load = Strength × Area. It is fully determined by the grain size G and specimen dimensions. Here, a_0 is the initial notch, S is the span of 3-p-b specimen, W is the width (or height), B is the thickness. The equivalent crack a_e is given as follows:

$$a_e = \left[\frac{\left(1-\alpha\right)^2 \cdot Y\left(\alpha\right)}{1.12}\right]^2 \cdot a_0 \tag{4}$$

This equivalent crack a_e has the following functions. A crack of 10 mm in a small specimen with size W = 15 mm is different to a crack of 10 mm in a large structure with size W = 1000 mm. Therefore, it is logical that Eq. (4) contains the geometry factor Y introduced in the critical stress intensity factor formula of LEFM, i.e. $K_{IC} = Y \cdot \sigma_c \sqrt{\pi \cdot a_0}$. The critical stress σ_c is influenced more by the ligament (W - a_0) than the notch length a_0 itself for the aforementioned small specimen with W = 15 mm. This is true for any deep-notched cases. The equivalent crack a_e is introduced to consider the influence from both the front and back specimen boundaries [6, 7]. a_e can approach to either a_0 or (W - a_0), depending on whether a_0 or (W - a_0) is smaller.

Why the tensile strength f_t criterion can also describe fracture initiated by a notch or crack, as indicated by Eq. (3)? This is because K_{IC} is fully determined by G and f_t.

$$K_{IC} = 2 \cdot f_t \cdot \sqrt{3 \cdot G} \qquad (5)$$

The above relation states the fracture toughness K_{IC} criterion is virtually the same as the tensile strength f_t criterion when the grain size G is considered in modeling. Therefore, f_t in Eq. (3) can describe quasi-brittle fracture cases with or without notch. Eq. (5) can be derived from Eq. (2) and the characteristic crack a^*_{ch} in [4, 7].

It should be mentioned that the equivalent area A_e in Eq. (3) is fully determined, and can be easily evaluated using an Excel spread sheet. Considering the relation between P_{max} and A_e in Eq. (3), we can expect a straight line with the tensile strength f_t as the slope, or one and only parameter needed. Therefore, quasi-brittle fracture of heterogeneous solids can be simply described by the linear relation between P_{max} and A_e. In other words, the linear BEM relation Eq. (3) is sufficient to describe non-LEFM events, such as quasi-brittle fracture of concrete and rock.

3 ANALYSIS OF GRANITE AND SANDSTONE DATA & MODELS

We selected a granite with the average grain size G around 2 mm and a medium-grained sandstone with G around 0.3 – 0.4 mm to illustrate how Eq. (3) can be used to analyse quasi-brittle fracture of rocks. Asphalt concrete results with the average aggregate size around 5 mm can be found in [15]. Concrete results with the maximum aggregate d_{max} from 10 to 40 mm can be found in [10]. That is the simplified BEM has been tested by various heterogeneous solids with G from 0.3 mm to d_{max} up to 40 mm.

3.1 Granite with G around 2 mm

Four groups of small three-point-bending (3-p-b) specimens with thickness B = 25 mm have been tested. 16 tests have been performed for each group [14]. The specimens are designated by notch, size and span/size ratio (group-a_0-W-S/W). They are g4-27-4, g6-27-4, g8-40-2.5 and g4-70-4. That is g4-27-4 with the initial notch a_0 of 4 mm, W = 27 mm, S/W = 4.

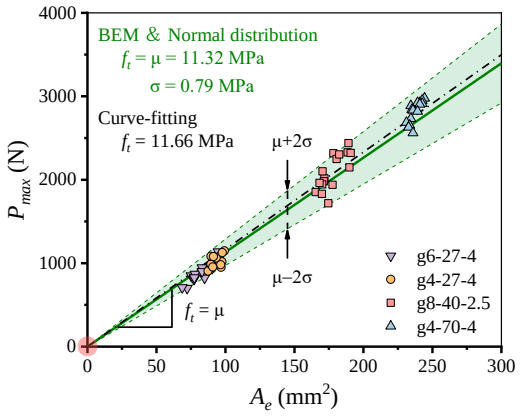

Figure 1: Predicted mean curve from Eq. (3), and the scatter band with 95% reliability for granite.

These four groups of specimens are not geometrically similar, as they differ either by the S/W ratio, or by the a_0/W ratio. Yet, they all can be analyzed together by Eq. (3), generating a single P_{max} and A_e relation as shown in Fig. 1, where the slope or tensile strength f_t = 11.32 MPa.

For every P_{max} measurement, a f_t value can be evaluated using Eq. (3). Those f_t values (i = 1, 2, 3…) are then used to evaluate the mean μ and standard deviation σ using the following normal distribution.

$$f\left[f_{t(i)}\right]=\frac{1}{\sqrt{2\pi}\sigma}e^{-\frac{\left[f_{t(i)}-\mu\right]^2}{2\sigma^2}} \quad (i=1, 2\cdots) \quad (6)$$

The tensile strength f_t in Eq. (3) can now be replaced by known $(\mu \pm 2\sigma) = (11.32 \pm 2\times0.793)$ so that.

$$P_{max}=(\mu\pm2\sigma)\cdot A_e(W,\ a_0,\ G)$$

$$=(\mu\pm2\sigma)\cdot\frac{W^2(1-\alpha)\left(1-\alpha+\frac{3G}{W}\right)}{1.5\left(\frac{S}{B}\right)\sqrt{1+\frac{a_e}{3G}}} \quad (7)$$

Now, the mean straight line and scatter band with 95% reliability can be predicted with given $(\mu \pm 2\sigma)$ values, as in Fig. 1. Common curve-fitting can also be used to analyze the data, but only the best fitted mean curve can be obtained, showing f_t= 11.66 MPa. The relative error between the normal distribution analysis and curve fitting is about 3%. However, the common curve-fitting practice cannot deal with the experimental scatters. Using the current normal distribution analysis, curve fitting is no longer needed.

The mean straight line in Fig. 1 goes through the origin (0, 0), which is also 100% accurate for Eq. (3). Since only two points are needed to determine a straight line, we only need to determine the 2nd point, or only need to do "one measurement". In principle, any specimen group can be selected since all are on the straight line as shown in Fig. 1. Group g4-27-4 is chosen here, and the result based on "one measurement" from g4-27-4 is shown in Fig. 2.

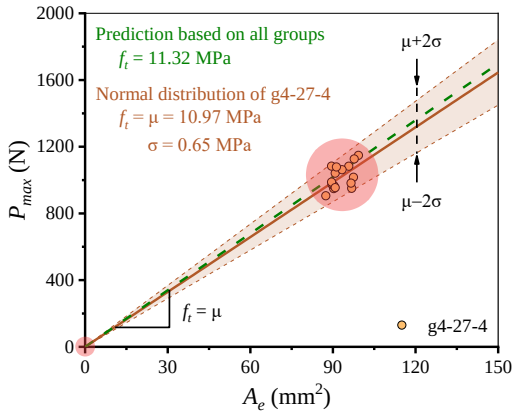

Figure 2: The linear relation based on "one measurement" from g4-27-4 specimens.

The tensile strength f_t based on this single group of tests is 10.97 MPa. It has only 3% error in comparison to the value of 11.32 MPa determined from all four groups. Therefore, the "one measurement" from one group of tests is plausible as long as the number of specimens tested is large enough, e.g. > 30.

It should be mentioned that the W/G ratio for the granite specimens is small, varying from 13.5 to 35. The a_0/G ratio is even smaller, varying from only 2 to 4. Therefore, those granite specimens are highly heterogeneous, and their fracture is quasi-brittle.

3.2 Sandstone with G around 0.3 – 0.4 mm

For simplicity, the mid value of G = 0.35 mm is used in this study. Different to the granite specimens, we have geometrically similar specimens for the sandstone. W = 30, 60, 100 and 300 mm, and the notch/size ratio, $\alpha = a_0/W$ = 0.2. Thickness B = 20mm, and the S/W ratio is 2.5.

Un-notched specimens with W = 10 mm, B= 20 mm, and S/W = 2.5 are also tested. The volume ratio of the largest specimen over the smallest specimen is 900. Both notched and un-notched results are analyzed together by Eqs. (6) & (7), and the results are shown in Fig. 3.

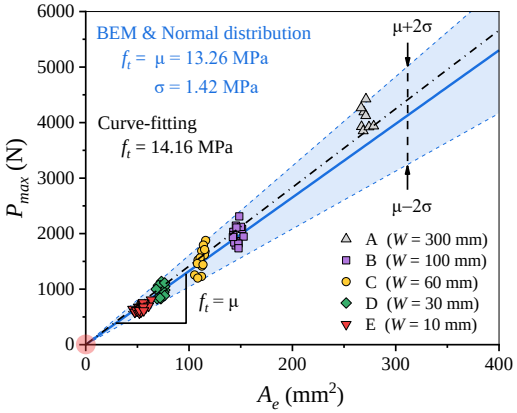

Figure 3: Predicted mean curve from Eq. (3), and the scatter band with 95% reliability for sandstone.

Only the largest specimens (W = 300 mm) appear to be away from the center line, but still within 95% reliability band. As B is only 20 mm, the tests of those "thin plates" are difficult to control. The typical BEM plot in Fig. 4 shows the error in the results of largest specimens is

still relatively small. With the W/G ratio of around 860 and a_0/G ratio of 170, fracture of the largest sandstone specimens can be approximately described by LEFM.

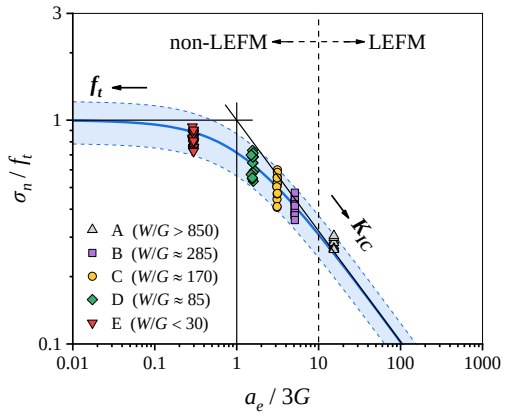

Figure 4: Typical BEM curve showing both f_t and K_{IC} asymptotic limits. Note that the largest specimens are close to the LEFM line (with about 10% error).

Special attention needs to be paid to the un-notched results. Cutting of specimens can easily break bonds of grains along the cutting surface and edges, creating an equivalent initial notch around G, depending on the bonding nature of rocks and cutting conditions. In this study, "$a_0 = G = 0.35$" has been assigned to the un-notched specimens.

3.3 One Parameter & One Measurement

Because of the highly heterogeneous material structures, it is known for a long time that fracture of concrete and rock is quasi-brittle and cannot be described by LEFM. The classic Hillerborg's fictitious crack-bridging model proposed in 1976 [11] for quasi-brittle fracture of concrete needs the specific fracture energy G_F and tensile softening relation, i.e. at least two parameters. The problem is that G_F is size dependent [16-19]. Besides 2P-SEL [3], there are others quasi-brittle fracture models, e.g. multi-fractal scaling law [20], which also contains two parameters. Therefore, it has been commonly accepted that LEFM needs one parameter K_{IC} to describe linear elastic fracture of ideally brittle homogeneous glass, non-LEFM models will need at least two parameters to describe quasi-brittle fracture of heterogeneous concrete and rock. The previous BEM [4-7] also contains two material constants f_t and K_{IC}.

The linear P_{max} - A_e relation in Eq. (3) or the simplified BEM goes through the origin (0, 0), which is 100% accurate theoretically. Since in principle only one more point is needed to fully determine the linear relation, the linear BEM has virtually become a "one-parameter (f_t)" and "one-measurement" non-LEFM model. However, this "one-parameter" and "one-measurement" model is fully capable of describing the complex quasi-brittle fracture of heterogeneous solids such as rock and concrete. The simplicity of this closed-form solution will be appreciated even more after one has tried SEL for quasi-brittle fracture modeling.

3.4 Three SELs & Three Different Trends

The simplest and most well-known SEL [3] is designed for deep-notched specimens, typically with α-ratio > 0.1.

$$\sigma_N = \frac{B_0 f_t'}{\sqrt{1+W/W_0}} \tag{8}$$

Here we use 2P-SEL for Eq. (8) since it contains two curve-fitting parameters B_0 and W_0. As shown in [1, 2], one curve-fitting is only for one α-ratio. If two groups of specimens with α = 0.1 and 0.2, two separate curve-fitting exercises are needed (as both B_0 and W_0 vary with α-ratio). The general trend of Eq. (8) is illustrated in Fig. 5.

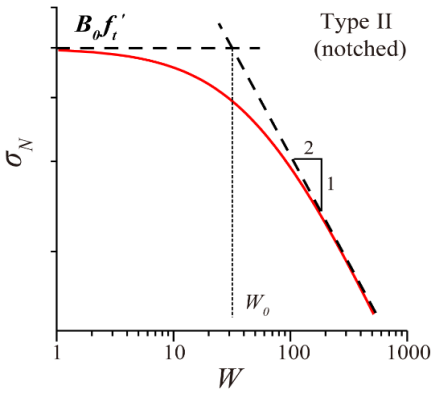

Figure 5: 2P-SEL for deep-notched specimens [23].

The two SELs for un-notched specimens are given below [1, 2, 21, 22] and their general trends are shown in Fig. 6.

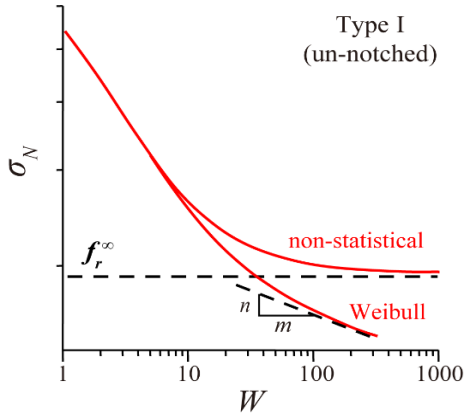

Figure 6: SELs for un-notched specimens [23].

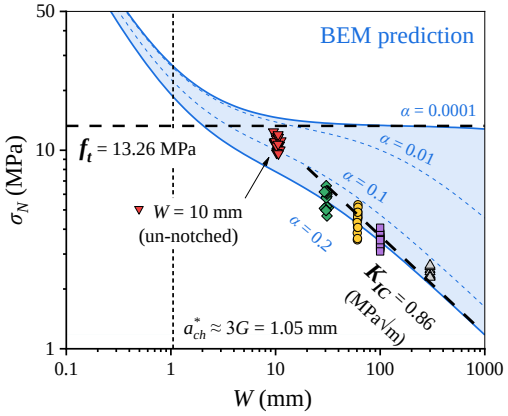

Figure 7: SEL curves predicted by Eq. (3).

$$\sigma_N = f_r^\infty \left(1 + \frac{rW_b}{W + l_p}\right)^{1/r} \quad (9)$$

$$\sigma_N = f_r^\infty \left[\left(\frac{W_b}{l_s + W}\right)^{rn/m} + \frac{rW_b}{l_p + W}\right]^{1/r} \quad (10)$$

Eq. (9) or 4P-SEL (4-parameters) is non-statistical as Weibull size effect is not considered. Eq. (10) or 7P-SEL (7-parameters) has considered the Weibull size effect, i.e. a bigger sample contains more defects (larger size as well) than a smaller sample [23]. Therefore, with increasing size W, the nominal strength σ_N is monotonically decreasing. However, in comparison with Eq. (7), Eq. (10) is not really statistical as it does not specify any statistical scatter band.

The biggest uncertainty of SEL is that two different tensile strengths, f_t and f_r^∞, are specified in Eqs. (7-9). Using f_t and K_{IC} results of the simplified BEM in Fig. 3, SEL curves have been predicted for various α-ratios and shown in Fig. 7 together with the experimental results. Note that σ_n in BEM considers the presence of notch a_0 while σ_N in SEL does not [4, 7]. The smallest un-notched specimens did not achieve the full tensile strength value of 13.26 MPa due to small pre-existing defects.

If α-ratio is approaching 0 (e.g. 0.0001), the SEL curve in Fig. 7 predicted by BEM is virtually the same as that of Eq. (9) with $f_t = f_r^\infty$ = 13.26 MPa. To the authors' best knowledge, this is the first time those two strengths in SEL are linked together. To some degree, the SEL curve with a small α-ratio, e.g. 0.01 in Fig. 7, is akin to that of Eq. (10) shown in Fig. 6. This is because within a limited size range, Weibull size effect is similar to SEL with a small α-ratio as discussed in [23].

For very small size W, BEM predictions in Fig. 7 are different to SEL with $\alpha > 0.1$ as shown in Fig. 5. Let us consider two groups of geometrically similar specimens with $\alpha = 0$ and 0.1. If size W is sufficiently small, the notch a_0 in the small specimens may be just a fraction of the aggregate size d_{max}. It means there is no difference between very small specimens [7]. Therefore, we believe the BEM predictions of SEL for very small W in Fig. 7 are correct.

Of course, 2P-SEL can also be used for curve-fitting of the sandstone results with α = 0.2. However, one has to assume a B_0 value before f_t can be estimated. 4P-SEL and 7P-SEL are seldom used as with more free parameters curve-fitting becomes less meaningful. In other words, un-notched specimens have not been dealt with convincingly by SEL.

4 DISCUSSION

4.1 Linear BEM & Fracture Prediction

The comprehensive concrete data initially reported in [9] can be quickly analyzed and predicted by Eq. (7). d_{max} of the concrete is 10 mm. Using the approximate relation between G and d_{max} given in Eq. (1), Eq. (7) can be rearranged using d_{max}. The BEM predictions together the P_{max} data are shown in Fig. 8.

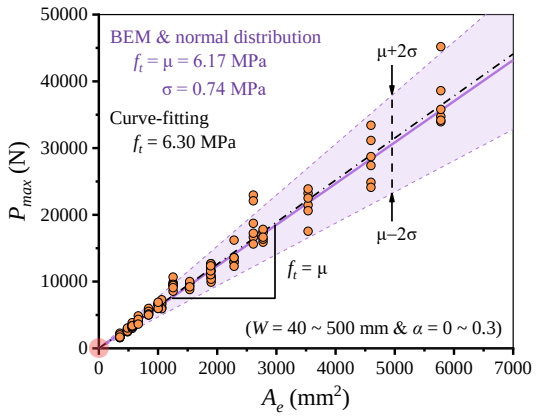

Figure 8: Prediction of quasi-brittle fracture of concrete with d_{max} = 10 mm [9] using Eq. (7) after replacing G with d_{max}.

This concrete example in Fig. 8 shows that the simple closed-form solution of BEM Eq. (3) has significantly simplified quasi-brittle fracture modeling of heterogeneous solids such as concrete and rock. After evaluation of test results using the normal distribution in Eq. (6), Eq. (7) becomes a predictive model, providing both the mean and 95% reliability band. The data shown in Fig. 8 has been collected from the most comprehensive concrete tests, as claimed in [1, 8, 9, 22] with α = 0, 0.025, 0.075, 0.15 and 0.3. In Fig. 8, those five different groups of geometrically similar specimens have been group together and well described by the linear BEM. In [10], K_{IC} is determined since both f_t and K_{IC} are interchangeable as indicated by Eq. (5). It should also be mentioned that those results with α = 0.025 and 0.075 cannot even be modeled by the three SELs, Eqs. (8-10). Two more universal SELs [1, 8, 9, 21, 22] have to be used for $0 < \alpha < 0.1$ as discussed in [7]. For the five different α values, 0, 0.025, 0.075, 0.15 and 0.3, five different fitted curves from at least three different SELs have to be used [7]. In contrast, the linear BEM with only the tensile strength f_t can predict all, as shown in Fig.8. Linearization of non-LEFM prediction of quasi-brittle fracture has significantly simplify size effect modeling. Furthermore, this linear relation goes through the origin (0, 0), making it become "simplest model" possible.

4.2 SEL & Curve-fitting

Due to its simplicity, 2P-SEL Eq. (8) is most widely used for curve-fitting. It can also be rearranged into a linear form, so that the two unknown parameters (2-P) can be determined from curve-fitting. The real problem is that both B_0 and W_0 determined from curve-fitting vary with α-ratio [1, 2, 7], which casts doubt on its applications in design and material property characterizations.

Furthermore, 2P-SEL is only limited to geometrically similar specimens with α = constant > 0.1. In contrast, the linear BEM in Eq. (3) can be used for both notched and un-notched specimens/structures whether they are geometrically similar or not.

5 CONCLUSIONS

A simple closed-form solution for quasi-brittle fracture of heterogeneous solids such as rock and concrete has been presented. This linear BEM is "one-parameter" strength criterion, but covers LEFM, classic strength criterion and quasi-brittle fracture. It also has all the intended functions of five SELs with more than 20 parameters [7]. The BEM predictions in Figs. 1-4, 7 and 8 provide convincing evidence.

For most research students and young researchers who need to understand non-LEFM events and analyze quasi-brittle fracture and associated size effect, a simple closed-form equation, which has only "one-parameter" and requires only "one-measurement", certainly helps. The linear BEM provides a welcoming choice in comparison with five SELs with 20 plus curve-fitting parameters. Besides, all SELs are limited to geometrically similar specimens with a constant α-ratio.

From the viewpoint of scientific research, the five SELs do provide detailed and sound mathematical considerations for complex issues of quasi-brittle fracture events, such as crack bridging and micro-damage, and associated size and shape effects. Therefore, they should be useful to those who are strong in mathematics and those who are more interested in mechanism and micro-mechanics studies. However, for practical design applications and university teaching, a simple closed-form solution will always have its position. It has taken a long 20-year period for BEM to develop into its present closed-form solution from its first unsophisticated FraMCoS appearance in 1998 [24]. Certainly, Bažant's seminal size effect paper in 1984 [3] has been inspiring, and the impact of SEL on the development of BEM is huge.

REFERENCES

[1] Hoover, C.G. and Bažant, Z.P., 2014. Comparison of the Hu-Duan boundary effect model with the size-shape effect law for quasi-brittle fracture based on new comprehensive fracture tests. *J. Eng. Mech. - ASCE.* **140**(3):480-486.

[2] Caglar, Y. and Sener, S., 2016. Size effect tests of different notch depth specimens with support rotation measurements. *Eng. Fract. Mech.* **157**:43-55.

[3] Bažant, Z.P., 1984. Size effect in blunt fracture: concrete, rock, metal. *J. Eng. Mech.* **110**(4):518-535.

[4] Hu, X. and Wittmann, F., 2000. Size effect on toughness induced by crack close to free surface. *Eng. Fract. Mech.* **65**(2-3):209-221.

[5] Hu, X. and Duan, K., 2008. Size effect and quasi-brittle fracture: the role of FPZ. *Int. J. Fract.* **154**(1-2):3-14.

[6] Wang Y., Hu, X., Liang, L., et al., 2016. Determination of tensile strength and fracture toughness of concrete using notched 3-pb specimens. *Eng. Fract. Mech*. **160**:67-77.

[7] Hu, X., Guan, J., Wang, Y., et al., 2017. Comparison of boundary and size effect models based on new developments. *Eng. Fract. Mech*. **175**:146–167.

[8] Hoover, C.G. and Bažant, Z.P., 2013. Comprehensive concrete fracture tests: size effects of types 1 & 2, crack length effect and postpeak. *Eng. Fract. Mech*. **110**:281-289.

[9] Hoover, C.G., Bažant, Z.P., Vorel, J., et al., 2013. Comprehensive concrete fracture tests: description and results. *Eng. Fract. Mech*. **114**:92-103.

[10] Guan, J., Yuan, P., Hu, X., et al., 2019. Statistical analysis of concrete fracture using normal distribution pertinent to maximum aggregate size, *Theor. Appl. Fract. Mech.* **101**:236-253.

[11] Hillerborg, A., Modéer, M. and Petersson, P.E., 1976. Analysis of crack formation and crack growth in concrete bymeans of fracture mechanics and finiteelements. *Cem. Concr. Res*. **6**(6):773-781.

[12] Zhang, C., Hu, X., Sercombe, T., et al., 2018. Prediction of ceramic fracture with normal distribution pertinent to grain size. *Acta Mater*. **145**:41-48.

[13] Zhang, C., Hu, X., Wu, Z. and Li, Q., 2018. Influence of grain size on granite strength and toughness with reliability specified by normal distribution. *Theor. Appl. Fract. Mech*. **96**:534-544

[14] Han, X., Chen, Y., Hu, X., et al., 2019. Granite strength and toughness from small notched three-point-bend specimens of geometry dissimilarity. Submitted to *Eng. Fract. Mech.* in February 2019.

[15] Wang, B., Hu, X, Ma, B., et al., 2019. Low temperature tensile strength and fracture toughness of asphalt concrete determined

from small notched 3-p-b specimens. In Proceedings of FraMCoS-X, France, June 24-26, 2019.

[16] Elices, M, Guinea, G.V. and Planas, J., 1992. Measurement of the fracture energy using three-point bend tests: Part 3 - Influence of cutting the P-d tail. *Mater. Struct.* **25:**137-163.

[17] Hu, X. and Wittmann, F., 1992. Fracture energy and fracture process zone. *Mater. Struct.* **25:**259-326.

[18] Cifuentes, H., Alcalde, M. and Medina, F., 2013. Measuring the size-independent fracture energy of concrete, *Strain* **49**:54-59.

[19] Karihaloo, B.L., Murthy, A.R. and Iyer, N.R., 2013. Determination of size-independent specific fracture energy of concrete mixes by the tri-linear model. *Cem. Concr. Res*. **49**:82-88.

[20] Carpinteri, A., 1994. Scaling laws and renormalization groups for strength and toughness of disordered materials. I*nter. J. Solids Struct.* **31**(3):291-302.

[21] Bažant, Z.P. and Yu, Q., 2009. Universal size effect law and effect of crack depth on quasi-brittle structure strength. *J. Eng. Mech*. **135**(2):78-84.

[22] Hoover, C.G. and Bažant, Z.P., 2014. Universal size-shape effect law based on comprehensive concrete fracture tests. *J. Eng. Mech. - ASCE*. **140**(3):473-479.

[23] Hu, X., Liang, L. and Yang, S., 2013. Weibull-strength size effect and common problems with size effect models. In Proceedings of FraMCoS-8, Spain 2013.

[24] Hu, X., 1998. Size effects in toughness induced by crack close to free edge. In Mihashi and Rokugo (eds), Fracture Mechanics of Concrete Structures; Proc. of the 3rd Inter. Conf. on Fract. Mech. Of Conc. and Conc. Struct. (FraMCos-3), October 12-16, 1998, Gifu, Japan; pp. 2011-20.